Mathematical modeling of volatile organic compounds removal over activated carbon

Yadollah Tavan [a, b], Hossein Bahmanyar [c*], Hedayat Azizpour [c, d+]

[a] *Chemical and Petroleum Engineering Department, Sharif University of Technology, Azadi Av., Tehran, Iran*
b Visiting researcher, Department of Chemical Engineering, Ecole Polytechnique de Montréal, Montréal, Québec, Canada
c Surface Phenomena and Liquid-Liquid Extraction Research Laboratory, School of Chemical Engineering, College of Engineering, University of Tehran, Tehran, Iran
d Department of Chemical Engineering, Fouman Faculty of Engineering, College of Engineering, University of Tehran, Iran

Abstract

Removal of volatile organic compounds (VOC) from air is essential due to health issues. An industrial cyclic temperature swing adsorption (TSA) unit is investigated over activated carbon. The comparison of industrial data with that of model showed good agreement between them. The results showed that ethanol is more adsorbed on activated carbon than diethyl ether and outlet concentration of diethyl ether exceeds its inlet concentration due to its partial replacement by ethanol. Performance of the TSA unit is measured through calculating diethyl ether and ethanol recoveries. Moreover, an energy requirement is also added into the model and multi-objective optimization has been carried out. High model accuracy of 99.98 % is obtained for objectives indicating a good fitting. The suggested optimum variables wereduration of heating stepas 30min, duration of cooling stepas 20 min, regeneration flow rate of 400 kmol/h and humidity of 0.001 in air.

Keywords: Multi-objective optimization, Ethanol, Diethyl ether, Mathematical model, Adsorption

*Corresponding author: Email address: hbahmany@ut.ac.ir (H. Bahmanyar).
+Corresponding author: Email address: h.azizpour@ut.ac.ir (H. Azizpour).

Introduction

Volatile organic compounds (VOCs) are some types of organic chemicals with high vapor pressure at room temperature.[1] VOC substances include alkanes, aromatics, ketones, paraffins, alcohols, esters, ethers and so on.[2]These hazardous chemicals are emitted from exhaust of industrial plants and involve in atmospheric photochemical reactions. Since these air pollutants cause long-term health problems and environmental issues, control of VOCs emission seems to be a major concern in quality of air. To control VOC emission into atmosphere, many technologies have been proposed such as biodegradation, condensation, catalytic oxidation, adsorption, absorption, etc. [3]When VOC high removal efficiency and good operation adaptation is concerned, the adsorption process is considered as an effective tool to treat VOCs. [4] In adsorption process, VOCs are held on surface of adsorbent and its pores using the vander Waals force. Activated carbon is widely used as a suitable adsorbent for VOCs recovery due to its large surface area, high adsorption capacity, non-selective nature and low cost comparing to zeolites. [5-6]However, activated carbon could not act as a catalyst properly and more appropriate adsorbent may be explored. When VOCs are passed over activated carbon, they are adsorbed on the carbon surface and treated air is exhausted to at atmosphere. When all surfaces of activated carbon are occupied, the adsorbent undergoes regeneration to release VOCs by heating it with steam in the temperature swing adsorption (TSA) system. As long as activated carbon gets warmer, it holds less VOCs and then the regeneration stream, a mixture of VOC and steam, exits from the bed and condensed. After cooling stage, the carbon is now ready to be re-used for adsorption.

Shah et al.,[7] investigated adsorption of acetone and methyl ethyl ketone (MEK) on activated carbon and its regeneration via hot air in a TSA system. They observed 95 % adsorption capacity for acetone at 80 °C and continuous degradation of the adsorption capacity for MEK. Wang et al.,[8] investigated adsorption process for automotive painting components on

beaded activated carbon and used hot nitrogen for desorption. They observed competitive adsorption for mixture and displacing of low boiling point compounds with high boiling point compounds. They found that high boiling point compounds may show "heel accumulation" on activated carbon due to their low desorption rate. Tefera et al.,[9] studied two-dimensionally model for adsorption of acetone, benzene, toluene and 1,2,4-trimethylbenzene in a fixed-bed cylindrical adsorber over beaded activated carbon. They investigated the effect of operating parameters (namely; temperature, superficial velocity, VOC load, particle size, etc) on the process efficiency and properly simulated transport phenomena in adsorber column. Kim et al., [10] used X- or Y-type Faujasite and Mordenite zeolites to adsorb VOCs and microwave heating for desorption. The highest adsorption capacity was attributed to Faujasite zeolite due to its large surface area and mesoporous volume. They finally concluded that pore structure of zeolites controls adsorption properties of zeolites. Wang et al., [11] synthesized a series of polymeric adsorbents to investigate dichloromethane and 2-butanon adsorption/desorption performance. They found that high surface area enhances adsorption of medium to high concentration of VOCs and meso-pores increase desorption efficiency. Al-Ghouti et al.,[12] characterized diethyl ether adsorption using an innovative refrigerator. They described adsorption data by the Langmuir model and chemisorption was attributed as the dominant mechanism for diethyl ether adsorption over activated carbon. An et al., [13] used the Grand Canonical Monte Carlo to simulate adsorption of VOCs on activated carbon. They found that although acetone and methanol can reach to their best adsorption capacity on activated carbon, benzene and toluene functional groups on reduces their adsorption performance. Laskar et al., [14]described competitive adsorption of water and multi-component of VOC over activated carbon. They properly fitted experimental data with that of model and proposed the modified Dubinin-Radushkevich and Qi-Hay-Rood models for VOCs and water vapor adsorption, respectively. Gabrus and Downarowicz[6] developed two combined TSA systems

for ethanol recovery from wet air over molecular sieve 3Aand activated carbon Sorbonorit-4.They utilized the Thomas model to predict breakthrough curve of ethanol and water in liquid and vapor phase.

Up to now, removal of VOCs is studied extensively and most of researchers only focused on adsorption state than cyclic one. In this study, industrial cyclic TSA unit is mathematically modeled to simultaneous removal of diethyl ether and ethanol from air. The breakthrough curves are plotted and compared to industrial data while good agreement is seen between them. With all progresses in modeling, simulation and optimization of TSA systems, there is a still shortcoming in multi-objective optimization. Based on open literature, there is scarce detail study attempting to model a TSA unit satisfying multi-objective optimization. Since, the regeneration step is the most important stage in the TSA unit, four variables relating to the regeneration step are considered as effective parameters. In order to reach the lowest operating costs and highest ethanol and diethyl ether recovery in the TSA unit, multi-objective optimization is conducted as a new study using the response surface methodology (RSM). Eventually, a set of regeneration variables and their optimal values are obtained and a model is proposed for individual objectives.

Mathematical model

A non-isothermal dynamic model is developed based on the following assumptions[15-17]:

- Axial dispersion-plug flow with radial changes in temperature and concentration being negligible.
- Given the pressure of the process under study, Peng-Robinson equation of state is utilized to describe gas parameters. Liquid properties are not discussed here.
- The linear driving force (LDF) governs the rate of adsorption and a lumped kinetic model is used for diffusion and adsorption into the particles.

- Bed wall is fully insulated.
- Pressure drop along bed obeys Ergun equation.
- Heat capacities are constant.
- Constant porosity of the bed along the column.

Mass balance of component i in the gas phase yields to:

$$\frac{\partial C_i}{\partial t} = D_{z,i}\frac{\partial^2 C_i}{\partial z^2} - U\frac{\partial C_i}{\partial z} - C_i\frac{\partial U}{\partial z} - (\frac{1-\varepsilon}{\varepsilon})\rho_p\frac{\partial q_i}{\partial t} \qquad \text{Eq. (1)}$$

Axial dispersion is determined as follows:

$$D_{z,i} = 0.73D_{m,i} + \frac{Ur_p}{\varepsilon_p(1+9.49\frac{\varepsilon_p D_{m,i}}{2Ur_p})} \qquad \text{Eq. (2)}$$

Effective diffusion is calculated as follows:

$$D_{m,i} = \frac{1-y_i}{\sum_j \frac{y_i}{D_{i,j}}} \qquad \text{Eq. (3)}$$

Molecular diffusion is computed as follows:

$$D_{i,j} = 1.01\times10^{-4}\times\frac{T^{1.5}}{P\sigma_{i,j}^2\Omega_D}(\frac{1}{M_i}+\frac{1}{M_j})^{0.5}\times[0.0027-0.0005(\frac{1}{M_i}+\frac{1}{M_j})^{0.5}] \qquad \text{Eq. (4)}$$

$$\Omega_D = [44.54\times(\frac{kT}{\varepsilon_{i,j}})^{-4.909}+1.911\times(\frac{kT}{\varepsilon_{i,j}})^{-1.575}]^{0.1} \qquad \text{Eq. (5)}$$

Overall mass transfer balance is as follows:

$$C_t\frac{\partial U}{\partial z} + (\frac{1-\varepsilon}{\varepsilon})\rho_p\sum_{i=1}^{n}\frac{\partial q_i}{\partial t} = 0 \qquad \text{Eq. (6)}$$

Solid phase micro-pore mass balance is described by LDF:

$$\frac{\partial q_i}{\partial t} = K_i (q_i^* - q_i) \qquad \text{Eq. (7)}$$

Overall mass transfer coefficient and its corresponding resistance are calculated as follows:

$$\frac{1}{K_i} = \frac{r_p}{3k_{f,i}} + \frac{r_p^2}{15\varepsilon_p D_{p,i}} \qquad \text{Eq. (8)}$$

Film mass transfer coefficient is calculated as follows:

$$Sh = \frac{k_{f,i} d_p}{D_{m,i}} = 2 + 1.1 Sc^{0.33} \mathrm{Re}^{0.6} \qquad \text{Eq. (9)}$$

Pore diffusivity of component i is:

$$D_{p.i} = \frac{\frac{1}{\tau}}{\frac{1}{D_{m,i}} + \frac{1}{D_{k,i}}} \qquad \text{Eq. (10)}$$

The Knudsen diffusion coefficient is:

$$D_{k.i} = 97 r_p \left(\frac{T}{M_i}\right)^{0.5} \qquad \text{Eq. (11)}$$

The tortuosity factor is computed as follows:

$$\tau = \varepsilon_p + 1.5(1 - \varepsilon_p) \qquad \text{Eq. (12)}$$

The pressure drop equation is:

$$\frac{\partial P}{\partial z} = -\left(\frac{1.5\times10^{-3}\mu(1-\varepsilon)^2 U}{d_p^2 \varepsilon^3}\right) + \left(\frac{1.75\times10^{-5}\rho_g (1-\varepsilon) U^2}{d_p \varepsilon^3}\right) \qquad \text{Eq. (13)}$$

Bulk phase (gas) energy balance is:

$$\varepsilon K_{ax}\frac{\partial^2 T}{\partial z^2}-U\rho_g C_{pg}\frac{\partial T}{\partial z}-\varepsilon\rho_g C_{pg}\frac{\partial T}{\partial t}-a_p(1-\varepsilon)h_i(T-T_s)=0$$
$$\rho_w C_{pw}\frac{\partial T_w}{\partial t}=\frac{4h_w}{(d_{out}^2-d_{in}^2)}(T_g-T_w) \qquad \text{Eq. (14)}$$

Solid phase (gas) energy balance is:

$$\rho_p C_{pp}\frac{\partial T_p}{\partial t}=\rho_p\sum_{i=1}^{n}(\Delta H_i)\frac{\partial q_i}{\partial t}+a_p h(T_g-T_p) \qquad \text{Eq. (15)}$$

Energy balance for wall thickness is calculated by:

$$\rho_w C_{pw}\frac{\partial T_w}{\partial t}=\frac{4h_w}{(d_{out}^2-d_{in}^2)}(T_g-T_w) \qquad \text{Eq. (16)}$$

The effective axial bed thermal conductivity is estimated as follows:

$$K_{ax}=K_g(7+0.5\mathrm{Pr}\,\mathrm{Re}) \qquad \text{Eq. (17)}$$

The extended Langmuir adsorption isotherm is used as follows:

$$\frac{q_i}{q_i^*}=\frac{IP_{1i}\exp(\frac{IP_{2i}}{T_s})P_i}{1+\sum_k(IP_{3k}\exp(\frac{IP_{4k}}{T_s})P_k)} \qquad \text{Eq. (18)}$$

Isotherm parameters of diethyl ether and ethanol are extracted from literature. [12,15]

All these governing equations are detailed elsewhere. [16-17] The governing equations are simultaneously solved using the finite difference method. To solve the equations, initial condition is assumed as:

$t=0 \quad \& \quad 0<z<L \qquad C_i=0 \quad T=293.15\ K$ Eq. (19)

Boundary conditions for mass and energy balance equations are as follows:

@z=0 $C_i=C_{inlet,i}$ and $T=T_{inlet}$ Eq. (20)

@ z=L $\frac{\partial C_i}{\partial z}=0$ and $\frac{\partial T}{\partial z}=0$ Eq. (21)

Process introduction

The TSA process includes four parallel adsorption beds in which three beds adsorb VOCs and one of them undergoes regeneration. The sequence of cyclic process and time for each steps are shown in Figure 1and Table 1.

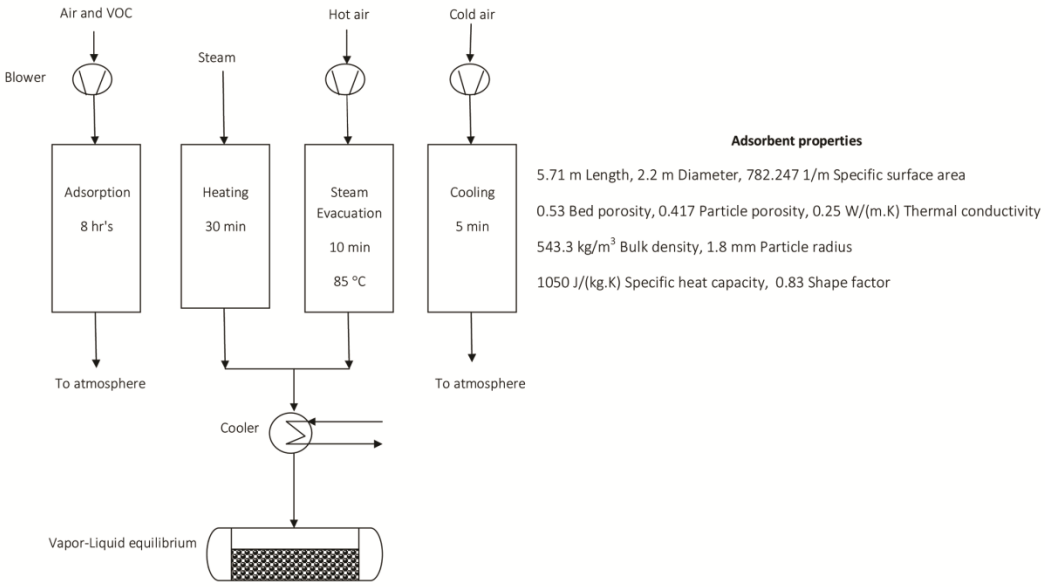

Figure1. The sequence of cyclic process

The cyclic process contains four steps namely adsorption, heating, evacuation and cooling with total time of 8 hr's and 45 minutes. Briefly, the polluted air passes through horizontal bed and VOCs are adsorbed on activated carbon surfaces and purified air is released into atmosphere. After adsorption stage, steam is utilized at 120°C to desorb VOC and then hot air evacuates/purges the adsorption bed from condensate water. The regenerated gas (air, steam,

condensate water and VOCs) are subjected to cooler for controlling its temperature. The remained gas is released into atmosphere and VOCs are now presented in liquid phase and they undergo further treatment while the adsorption bed is finally cooled via cold air.

Table 1. Properties of feed stream and adsorption stages

Property / Stage	Adsorption	Regeneration		
		Heating	Steam Evacuation	Cooling
Flow rate (kmol/h)	255	500	462.93	462.93
Temperature (°C)	20	120	85	20
Pressure (bar)	1.1	Saturated	1.1	1.1
Duration (min)	480	30	10	5
		Mole-fraction		
Air	0.9983	-	1	1
Water	0	1	-	-
Ethanol	0.0012	-	-	-
Diethyl Ether	0.0005	-	-	-

Table 2 demonstrates thermodynamic properties of components in which the process includes four components and two homogeneous azeotropes are shown in Figure 2a. Hence, more caution is needed when the regeneration gas is cooled down.

Table 2. Properties of components in the system

Properties / Component	Water	Air	Ethanol	Diethyl ether
Chemical Formula	H_2O	(21%)O_2/(79 %)N_2	C_2H_6O	$C_4H_{10}O$
Normal boiling point (°C)	100.02	-194.50	78.16	34.39
Molecular weight	18.02	28.95	46.07	74.12

Azeotropes classification

No.	Temperature (°C)	Classification	Type	Mole fraction		
				Diethyl Ether	Ethanol	H_2O
1	34.185	Unstable node	Homogeneous	0.957	0.000	0.043
2	78.164	Saddle	Homogeneous	0.000	0.900	0.100

The highest temperature is related to water and the lowest temperature is attributed to diethyl ether (ether)/water system. The ternary diagram and residue curve mapare shown in Figure 2b. These charts are extracted using the UNIQUAC thermodynamic model in Aspen plus simulation software for the pressure of 1 atm. The ternary diagram shows location of azeotropes and a liquid-liquid envelope in the system in which the ether/water azeotrope lies closely to the boundaries of this envelope. The azeotropes limit separation of component in single distillation column and more complicated process is needed to separate components. Hence, selection of suitable thermodynamic model is important when accurate vapor/liquid/liquid separation is desired. The tie-lines in the residue curve map are initiated from the lowest temperature and sloped toward the highest temperature (water), in which a stream containing water with small content of ethanol is recovered in the process.

Results and discussions

To validate the model, the breakthrough experiments are performed. Figure 3 compares experimental data received from industrial plant versus modeling results and fairly good agreement is seen between them. Accordingly, the model employed here adequately demonstrates dynamic behavior of adsorption bed and validity of the model is confirmed along with the considered assumptions. So, the results can be used as a useful tool for optimization of the TSA process in order to obtain highest performance (purity, recovery or etc).

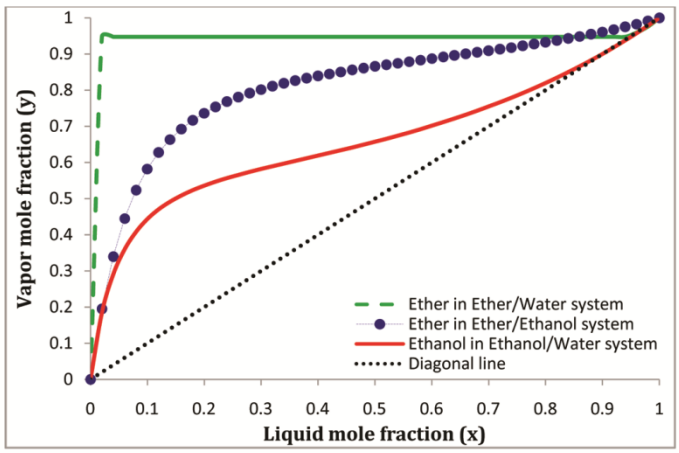

(a)

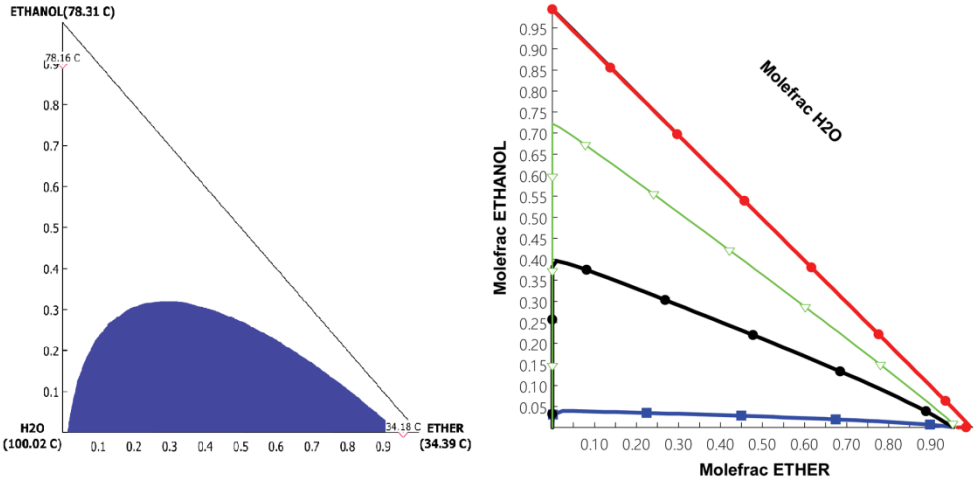

(b)

Figure2. The thermodynamic diagrams for the system in terms of (a) x-y diagram and (b) ternary and residue curve map

Figure 4 plots components and temperature profile for the system under study. Figure 4a shows that as time progresses, ethanol and diethyl ether are adsorbed on activated carbon surface and no comparable VOCs is seen in outlet of the bed. As time proceeds, more VOCs are presented in outlet of the bed and finally all surfaces of activated carbon are equipped and it no longer adsorbs impurities. Then, breakthrough happens and the bed saturates till same input and output concentration for VOCs is seen. Before breakthrough happening, the adsorption stage should be terminated and regeneration of activated carbon should be conducted. For mixture adsorption, it is seen that ethanol is more adsorbed on activated

carbon than diethyl ether under same adsorption condition and accordingly, ethanol breakthrough happen after diethyl ether.

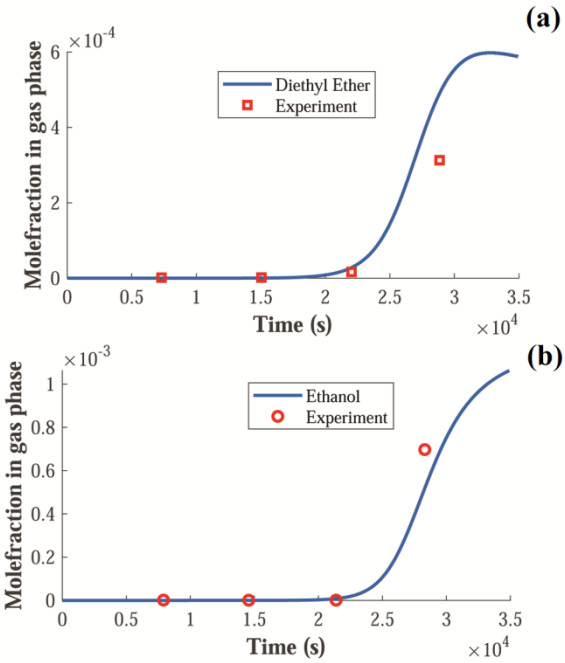

Figure3. Comparison between experimental data and model for (a) diethyl ether and (b) ethanol for feed flow rate of 333 kmol/h

Figure 4a also shows that outlet concentration of diethyl ether exceeds its inlet concentration due to its partial replacement by ethanol. This phenomenon which is called "Roll-up" refers to the humps on the diethyl ether breakthrough curve where its concentration exceeds the feed condition. [18] According to the Yang book [18], the "Roll-up" happens due to displacement of weaker adsorbate (diethyl ether) by a strong one (ethanol). In the beginning of adsorption, both diethyl ether and ethanol are adsorbed on activated carbon surfaces since there are enough empty adsorption site on the adsorbent. Figure 4b shows an interval of bed when surface of activated bed is covered by ethanol and diethyl ether, further adsorption of ethanol would replace the adsorbed diethyl ether so, desorption of diethyl ether happens and competitive adsorption behaviors exists in the bed intervals. Figure 4c shows that temperature

of gas stream is increased due to the nature of exothermic adsorption process till bed saturation and then no more heat is released in which gas temperature reaches to the feed temperature.

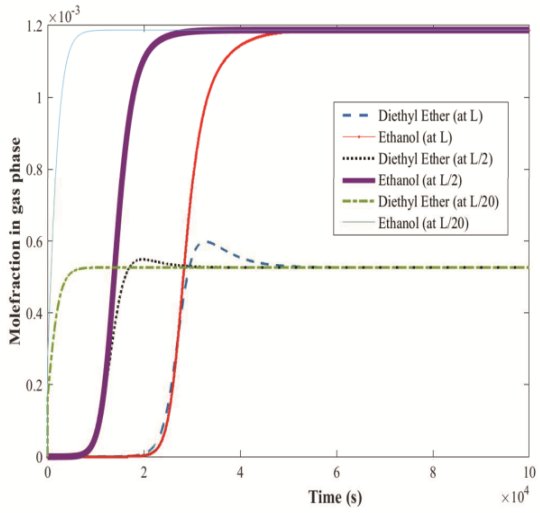

(a)

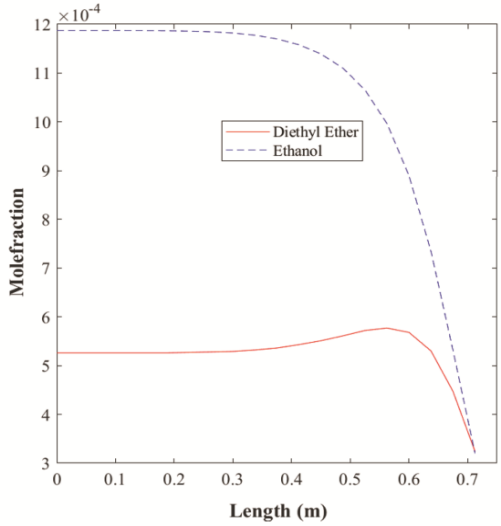

(b)

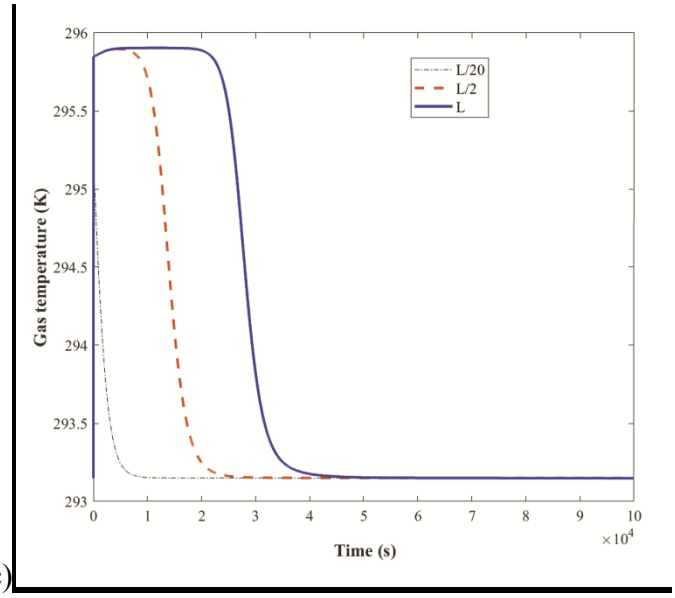

(c)

Figure4. Out-put of model in terms of (a) concentration of ethanol and diethyl ether as a function of time, (b) time interval of 27000 s for concentration of ethanol and diethyl ether as a function of adsorbent length and (c) temperature profile variation versus time at different length of bed for feed flow rate of 333 kmol/h

One of effective parameters in design of adsorption bed is gas superficial velocity. For constant feed flow rate, one can easily calculate diameter of adsorption bed based on gas velocity and feed flow rate. In adsorption processes, it is evident that gas superficial velocity greatly enhances energy and mass transfer by decreasing the external film around the adsorbent. [19]Increase in superficial velocity is favored till meeting maximum permissible pressure drop, near to the criterion of 7.50kPa/m. [17, 20]Figure 5 shows variation of Reynolds number, the Peclet number and velocities with time.

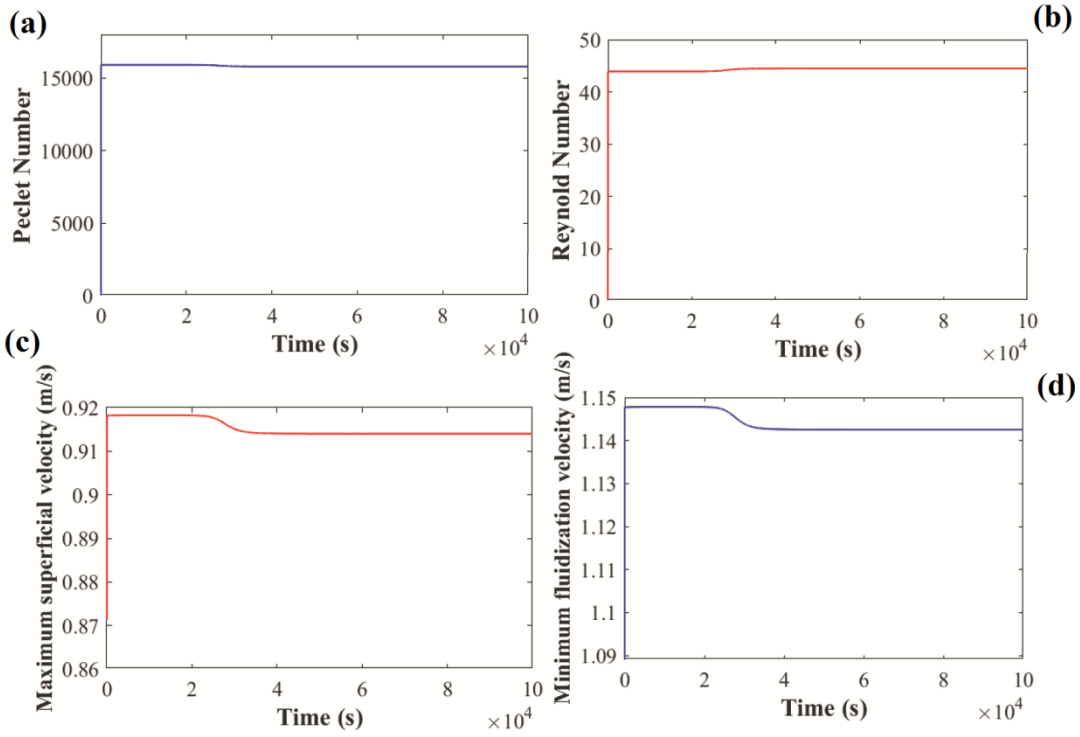

Figure5. Variation in (a) the Peclet number, (b) the Reynolds number, (c) maximum superficial velocity and (d) minimum fluidization velocity with time for feed flow rate of 333 kmol/h

The Peclet number quantifies the degree of dispersion introduced into the system. It is dimensionless so is more convenient than the dispersion coefficient for this purpose. A high value for the Peclet number in Figure 5a reveals that an assumption made for ignoring radial distribution of temperature and concentration is reasonable and the bed operates under plug

flow conditions. Since the adsorption unit is of horizontal bed type, the Reynolds number is small, as depicted in Figure 5b. Figure 5c and d also indicates that maximum superficial velocity is kept below the minimum fluidization velocity in horizontal adsorption unit. According to Figure 5, no significant change in the Peclet number, Reynolds number and velocities is observed after entrance of adsorption bed.

Industrial plant operates in a cyclic manner and after conducting several cycles, the adsorption process approaches to a cyclic steady state. Determining the required time to reach steady state cyclic process is typically performed by iteration method. [21] Figure 6 gives the simulation results in which cyclic steady state is established after three sequential running cycles in the process due to using high regeneration flow rate. Since most of feed (air) is not adsorbed on adsorbents, only few cycles is required to reach stable condition and this matter is in good agreement with literature. [22]Figure 6 shows that unsteady state conditions are raised due to temperature change and accumulation of energy in the bed. [22] The identical component profile is observed after three cyclic processes in Figure 6a and 6b. Figure 6c shows that identical temperature is occurred in adsorption bed.

Performance of TSA unit

Recovery of VOCs is of importance since they cause health problems. In order to investigate performance of the TSA unit, recovery of diethyl ether and ethanol is measured via equation 22. The recovery in equation 2 is defined as the amount of recovered ethanol/ diethyl ether during regeneration step divided by amount of ethanol/ diethyl ether in adsorption step.

$$\text{Recovery}\ (\%) = \frac{\int_{0}^{\text{Regeneration}} c_i v\big|_{z=L}\, dt}{\int_{0}^{\text{Adsorption}} c_i v\big|_{z=0}\, dt} \qquad \text{Eq. (22)}$$

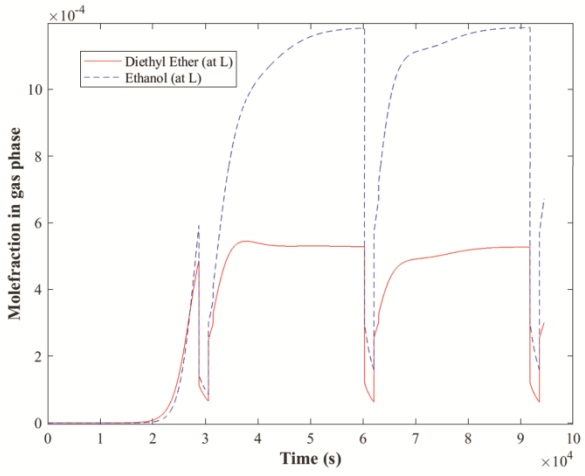

(a)

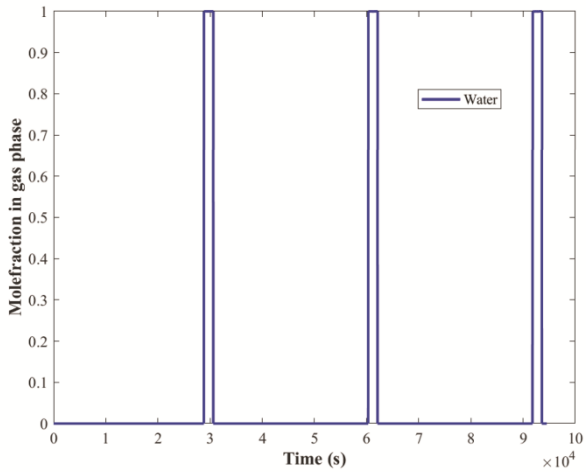

(b)

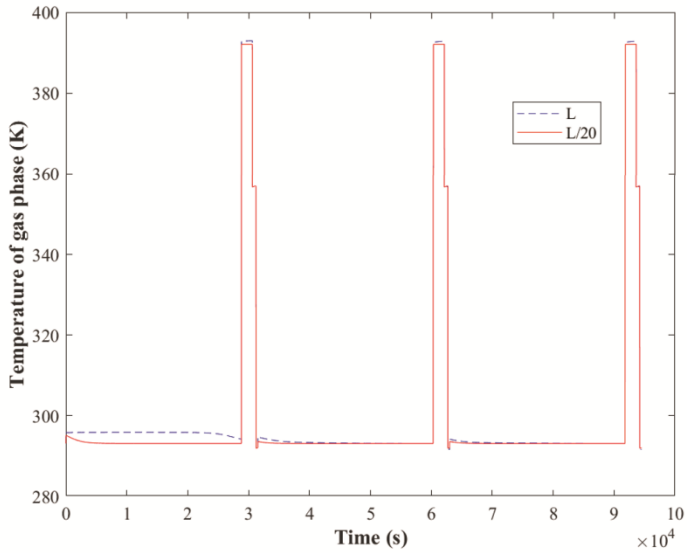

(c)

Figure6. Reaching to cyclic steady state condition for (a) ethanol and diethyl ether profiles, (b) water (steam) distribution and (c) temperature profile with time for feed flow rate of 333 kmol/h

Operating costs for the TSA unit

According to Figure 1, operating costs involves electrical energies in blowers to boost pressure of streams from ambient pressure to 2bar-g (during the adsorption, steam evacuation

and cooling stages) and flow rate of steam consumed during heating stage. Electrical energy required for all blowers are calculated using the Aspen HYSYS process simulator by implementing equations 23-25. This electrical energy (kJ/h) is then converted to "kW.h" by considering duration of adsorption, steam evacuation and cooling stages. The electrical energy cost per each cycle is computed as $ 0.1 per "kW.h". [23]

$$W=F_1(M_w)\left(\frac{n}{n-1}\right)CF\left(\frac{P_1}{\rho_1}\right)\left[\left(\frac{P_2}{P_1}\right)^{\left(\frac{n}{n-1}\right)}-1\right] \quad \text{Eq. (23)}$$

The volume exponent is calculated as:

$$n=\frac{\ln\left(\frac{P_2}{P_1}\right)}{\ln\left(\frac{\rho_2}{\rho_1}\right)} \quad \text{Eq. (24)}$$

The correction factor is calculated as:

$$CF=\frac{h_2-h_1}{\left(\frac{n}{n-1}\right)\left(\frac{P_2}{\rho_2}-\frac{P_1}{\rho_1}\right)} \quad \text{Eq. (25)}$$

The amount of steam consuming in the heating stage at the pressure of 2bar-g is converted to "tone" by considering duration of heating stage. The price of low pressure steam is calculated by considering $ 13 per "tone" of steam. [23]

Figure 7 clearly shows that the cost of using steam and electrical energies are 65% and 35% of total operating costs per each TSA cycle, in average. Hence, cost of steam has a great impact on total operating costs comparing to electrical energy.

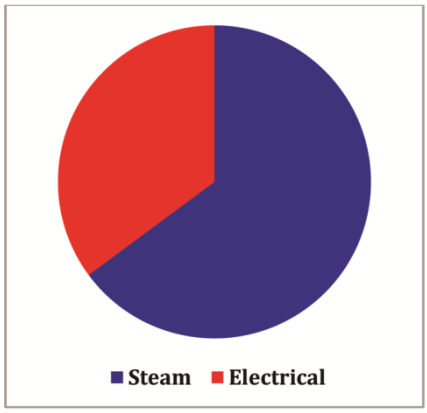

Figure7. The average contribution of utilities cost from total operating costs

Multi objective optimization

In most of previous studies, only adsorption step has been carried out to investigate the effect of different parameters on the adsorbent performance. Optimization of the TSA unit in terms of energy requirements and performance of the process appears as a good deal for VOC removal technologies. Accordingly, a model is required to describe the effect of process variables on recovery of VOCs and operating costs. After preliminary tests and in the fixed feed condition, duration of heating step (A), duration of cooling step (B), regeneration flow rate (C) and humidity of air (D) are considered as effective variables and their practical range are identified in Table 3. In this study, the Design-expert® software is utilized via the central composite design (CCD) method through performing 30 tests with five levels for each variable. Table 3 shows corresponding results for VOCs recoveries and operating costs per each cycle. The RSM proposed a 2FI correlation to relate diethyl ether recovery, ethanol recovery and operating costs to the independent variables. The results of analysis of variance showed that the P values for all three objectives are lower than 0.05 indicating that the model terms are significant and have significant effects because of the large F value. The large F-value showed that the model is significant while only 0.01 % chance that a "Model F-Value"

with this large F value could occur due to noise. Values of "Prob>F" less than 0.05 indicate that the model terms are significant. The results of the diethyl ether and ethanol recoveries showed thatincrease in the variable B leads to increase in diethyl ether recovery while increase in the variables A, C and D results in decrease in diethyl ether and ethanol recoveries. Increase in parameters C, A and B directly increase operating costs and increase in parameter D leads to lower operating cost.The model accuracy for all objectives has been higher that 99.98 % (R^2) indicating a good fitting of the correlation with the data. "Adeq Precision" measures the signal to noise ratio. A ratio greater than 4 is desirable. In this study, the “Adeq Precision” ratio higher than 103 is obtainedwhich indicates an adequate ratio. Also the “Adj R-Squared” is highe than 99.69 % which is close to “R-Squared” indicating a good accuracy of model. This model can be used to navigate the design space. Equations 26-28 show the empirical correlation for each objectives obtained by the RSM.

Diethyl ether cyclic recovery (%)=+84.88123+0.076377×A+0.24750×B+0.012657×C-685.03606×D-3.09525E-003×A×B-6.63543E-004×A×C+7.02308×A×D+1.54004E-004×B×C+7.04970×B×D+0.68891×C×D Eq. (26)

Ethanol cyclic recovery (%)=+63.86180+0.059023× A +0.16952×B +0.011428×C-299.78004×D-2.82108E-003×A×B-6.03091E-004×A×C+3.07032×A×D+4.22973E-004×B×C+3.09206×B×D+0.30129×C×D Eq. (27)

Operating costs ($)=-7.23003E-004+0.000000×A+4.81994E-005×B+0.029585×C+0.24099×D+0.000000×A×B+3.90000E-003×A×C+1.74583E-012×A×D+2.95818E-003×B×C-0.016066×B×D-8.92557E-004×C×D Eq. (28)

The predicted versus actual data for all three objectives confirmed that the predicted values of the model were in a good agreement with the given data.Figure 8 shows three-dimensional plot for interaction of variables on the objectives. The plot given in Figure 8 is easy-reading and straightforward in which a linear surface is seen between the independent parameters on the responses.

Table 3. Upper and lower bounds for variables with 255 kmol/h feed and the results

Run#	Heating time (min)	Cooling time(min)	Regeneration flow rate (kmol/h)	Humidity (mole fraction in air)	Diethyl ether cyclic recovery	Ethanol cyclic recovery	Total operating cost ($)
1	35	15	350	0.003	86.479	65.682	73.659
2	45	15	450	0.003	83.388	63.017	112.254
3	40	10	500	0.004	82.996	62.564	107.580
4	25	15	450	0.003	88.449	67.981	77.155
5	40	10	400	0.002	84.066	63.328	86.066
6	35	25	450	0.003	88.138	68.201	108.016
7	40	10	400	0.004	84.067	63.328	86.065
8	40	10	500	0.002	82.997	62.565	107.582
9	35	15	450	0.003	85.877	65.448	94.705
10	40	20	500	0.004	85.301	65.368	122.372
11	30	10	400	0.004	85.685	65.185	70.465
12	40	20	500	0.002	85.302	65.369	122.373
13	40	20	400	0.002	86.088	65.671	97.899
14	35	15	450	0.003	85.877	65.448	94.705
15	35	15	450	0.003	85.877	65.448	94.704
16	35	15	450	0.003	85.877	65.448	94.704
17	30	20	500	0.002	88.173	68.234	102.87
18	35	15	450	0.003	85.877	65.448	94.704
19	30	10	500	0.002	85.686	65.185	88.082
20	30	10	400	0.002	86.244	65.431	70.466
21	35	15	450	0.003	85.877	65.448	94.705
22	30	20	400	0.002	88.425	67.971	82.299
23	35	15	450	0.001	85.881	65.449	94.705
24	30	10	500	0.004	85.685	65.185	88.081
25	40	20	400	0.004	86.093	65.673	97.898
26	35	15	450	0.005	85.877	65.448	94.704
27	35	5	450	0.003	83.638	62.839	81.393
28	35	15	550	0.003	85.156	65.149	115.750
29	30	20	500	0.004	88.173	68.234	102.872
30	30	20	400	0.004	88.425	67.971	82.298

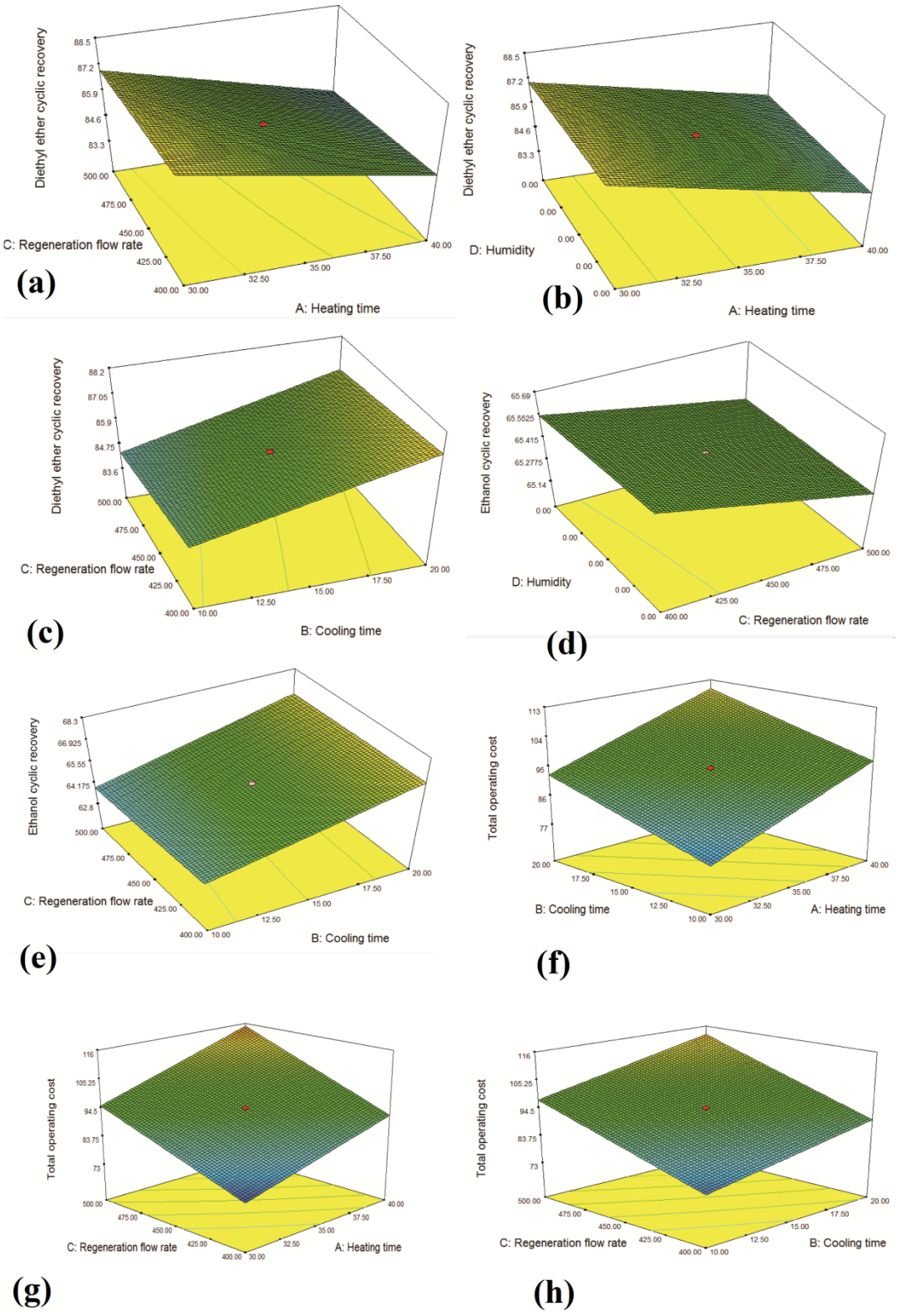

Figure 8. Interaction between parameters in terms of (a) A×C (for diethyl ether cyclic recovery), (b) A×D (for diethyl ether cyclic recovery), (c) B×C (for diethyl ether cyclic recovery), (d) D×C (for ethanol cyclic recovery), (e) B×C (for ethanol cyclic recovery), (f) A×B (for total operating), (g) A×C (for total operating), (h) B×C (for total operating)

Table 4 shows the optimal results for only one response. For multi-objective optimization, simultaneously recovery of diethyl ether and ethanol are set to maximum while minimum operating cost is desired. Last row in Table 4 shows theoptimal conditions for all three objectives using the Design expert® software.

Table 4. Results of single and multi objective optimization

Objective	Heating time (min)	Cooling time(min)	Regeneration flow rate (kmol/h)	Humidity	Diethyl ether cyclic recovery (%)	Ethanol cyclic recovery (%)	Total cost
Maximize Diethyl ether cyclic recovery	30.02	19.99	406.42	0.001	**88.45**	68.00	83.64
Maximize Ethanol cyclic recovery	30.00	20.00	498.07	0.001	88.21	**68.24**	102.48
Minimize Total cost	30.00	10.00	400.00	0.001	85.97	65.30	**70.47**
Multi-objective	30.00	20.00	400.00	0.001	**88.46**	**67.99**	**82.29**

The suggested optimum variables are: heating time of 30min, cooling time of 20 min, regeneration flow rate of 400 kmol/h and humidity of 0.001 in air. Based on the results of optimization path given in Figure 9when decrease in total operating costs and increase in recovery of VOCs is desired, one can conculde that:

- Duration of heating stage should keep low as practicaly possible.
- Duration of cooling stage should be large enough.
- The small flow rate for regeneration and low humidity in air is desired.

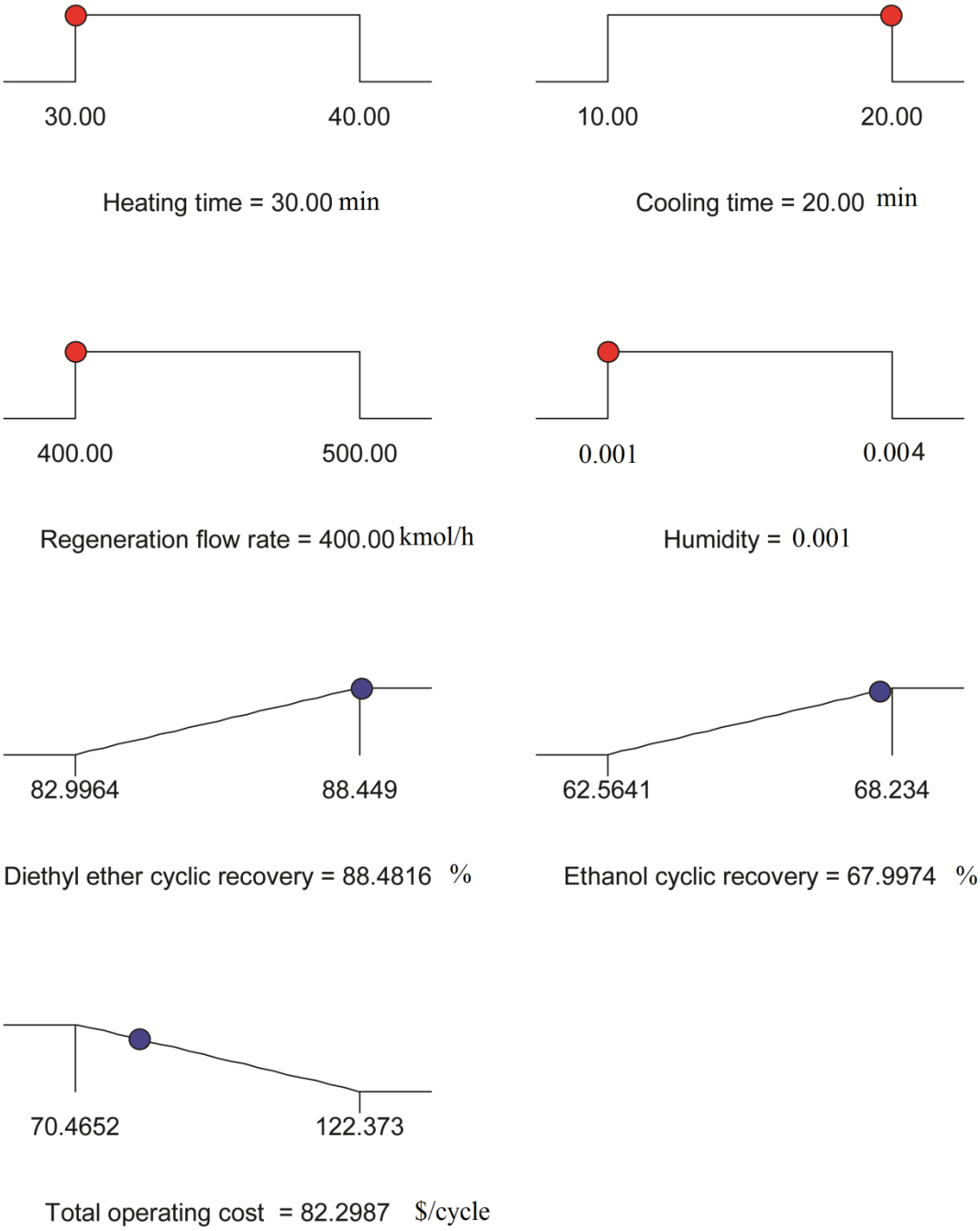

Figure 9. The optimization path

Conclusion

An industrial cyclic temperature swing adsorption (TSA) unit is investigated to study VOC removal from air stream. Thermodynamic properties of components showed that the process includes four components and two homogeneous azeotropes. Therefore, cooling of the regeneration gas must be carried out with care. The results of TSA unit showed that ethanol is strongly adsorbed on activated carbon than diethyl ether and ethanol replace adsorbed diethyl ether so, the concentration of diethyl ether exceeds from its feed condition. The results of mathematical modeling also showed that the Peclet number is large enough (near 15000) and the adsorption bed can be considered as the plug flow conditions. The dynamic VOC adsorption in the TSA unit showed that three cycles is required to reach steady state. To perform optimization study, four parameters namely duration of heating step (A), duration of cooling step (B), regeneration flow rate (C) and humidity of air (D) have been considered on maximizing diethyl ether and ethanol recovery and minimizing operating costs. In the optimal condition, duration of heating stepwas 30min, duration of cooling stepwas20 min, regeneration flow rate was 400 kmol/h and humidity was 0.001 in air.

References

1.Khan FI, Ghoshal AK. Removal of volatile organic compounds from polluted air. J Loss Prevent Process Ind. 2000; 13: 527-545.

2.Talmoudi R, Jaoued AA, Chahbani MH. Dynamic study of VSA and TSA processes for VOCs removal from air. Int J Chem Eng. 2018 ; https://doi.org/10.1155/2018/2316827.

3.Yang C, Miao G, Pi Y, Xia Q, Wu J, Li Z, Xiao J. Abatement of various types of VOCs by adsorption/ catalytic oxidation: A review. Chem Eng J. 2019; 370: 1128-1153.

4. Sui H, Liu J, He L, Li X, Jani A. Adsorption and desorption of binary mixture of acetone and ethyl acetate on silica gel. Chem Eng Sci.2019; 197: 185-194.

5. Swetha G, Gopi T, Shekar SC, Bijendra Saini CR, Rao PVL. Combination of adsorption followed by ozone oxidation with pressure swing adsorption technology for the removal of VOCs from contaminated air streams. Chem Eng Res Des.2017; 117: 725-732.

6. Gabrus E, Downarowicz D. Anhydrous ethanol recovery from wet air in TSA systems-Equilibrium and column studies. Chem Eng J. 2016; 288: 321-331.

7. Shah IK, Pre P, Alappat BJ. Effect of thermal regeneration of spent activated carbon on volatile organic compound adsorption performances. J Taiwan Inst Chem Eng. 2014; 45: 1733-1738.

8.Wang H, Jahandar Lashaki M, Fayaz M, Hashisho Z, Philips JH, Anderson JE, Nichols M. Adsorption and desorption of mixtures of organic vapors on beaded activated carbon. Environ Sci Technol.2012; 46: 8341-8350.

9. Tefera DT, Lashaki MJ, Fayaz M, Hashisho Z, Philips JH, Anderson JE, Nichols M. Two-dimensional modeling of Volatile Organic Compounds adsorption onto beaded activated carbon. Environ. Sci Technol.2013; 47: 11700-11710.

10.Kim K-J, Ahn H-G. The effect of pore structure of zeolite on the adsorption of VOCs and their desorption properties by microwave heating. Micropor Mesopor Mater.2012; 152: 78-83.

11.Wang S, Zhang L, Long C, Li A. Enhanced adsorption and desorption of VOCs vapor on novel micro-mesoporous polymeric adsorbents. J Colloid Interface Sci.2014; 428: 185-190.

12. Al-Ghouti MA, Yousef I, Ahmad R, Ghrair AM, Al-Maaitah AA. Characterization of diethyl ether adsorption on activated carbon using a novel adsorption refrigerator. Chem Eng J. 2010; 162: 234-241.

13.An Y, Fu Q, Zhang D, Wang Y, Tang Z. Performance evaluation of activated carbon with different pore sizes and functional groups for VOC adsorption by molecular simulation. Chemosphere. 2019; 227:9-16.

14.Laskar II, Hashisho Z, Phillips JH, Anderson JE, Nichols M. Competitive adsorption equilibrium modeling of Volatile organic compound (VOC) and water vapor onto activated carbon. SepPurif Technol. 2019; 212:632-640.

15.Bouzid M, Sellaoui L, Khalfaoui M, Belmabrouk H,. Lamine AB. Adsorption of ethanol onto activated carbon: Modeling and consequent interpretations based on statistical physics treatment. Physic A: Statist MechAppl. 2016; 444: 853-869.

16. TavanY, Hosseini SH, Olazar M. A note on integrated process of methane steam reforming in junction with pressure-swing adsorption to produce pure hydrogen: Mathematical modeling. Ind Eng Chem Res.2015; 54: 12937-12947.

17. Tavan Y, Hosseini SH, Ahmadi G, Olazar M. Mathematical model and energy analysis of ethane dehydration in a two-layer packed Bed Adsorption. Particu. 2019; 47: 33-40.

18.Yang RT, Gas separation by adsorption processes. Butterworth, 1987.

19.Sheikh Alivand M, Farhadi F. Multi-objective optimization of a multi-layer PTSA for LNG production. J Nat Gas Sci Eng. 2018; 49; 435-446.

20. GPSA data book, 2004.

21. Nastaj J, Ambrozek B. Analysis of gas dehydration in TSA system with multi-layered bed of solid adsorbents. Chem Eng Process. 2015; 96: 44-53.

22. Taheri Qazvini O, Fatemi S. Modeling and simulation pressure–temperature swing adsorption process to remove mercaptan from humid natural gas; a commercial case study. Sep Purif Technol. 2015; 139: 88-103.

23. Cong H, Murphy JP, Li X, Li H, Gao X. Feasibility evaluation of a novel middle vapor recompression distillation column. Ind Eng Chem Res. 2018; 57: 6317-6329.

Nomenclature:

a_p: Surface area of the adsorbent particle (1/m)

C_i : Concentration of component i in the gas phase (kmol/m^3)

C_{pg}: Heat capacity of the gas (kJ/kg/K)

C_{pp}: Heat capacity of the adsorbent particle (kJ/kg/K)

C_{pw}: Heat capacity of the wall (kJ/kg/K)

C_t : Total concentration of component i in the gas phase(kmol/m^3)

CF: Correction factor

$D_{j,i}$: Molecular diffusivity of j in i (m^2/s)

$D_{p,i}$: Pore diffusivity of component i (m^2/s)

$D_{k,i}$: Knudsen diffusivity of component i (m^2/s)

$D_{m,i}$: Molecular diffusivity of component i in the mixture (m^2/s)

$D_{z,i}$: Effective axial dispersion coefficient of component i (m^2/s)

d_p: Adsorbent particle diameter (m)

d_{in}/d_{out}:Inner diameter/ outer diameter (m)

F1: Molar flow rate of the inlet stream

h_i: Heat transfer coefficient in gas phase (W/m^2/K)

h_w: Heat transfer coefficient between wall and bed (W/m^2/K)

h_2: Enthalpy of the exit stream corresponding to the inlet entropy

h_1: Enthalpy of the inlet stream

IP_i: Langmuir adsorption parameters

K_{ax}: Effective axial thermal conductivity (W/m/K)

K_g: Thermal conductivity of the gas mixture (W/m/K)

K_i: Overall mass transfer coefficient of component i (1/s)

$K_{f,i}$: Outer mass transfer coefficient of component i (m/s)

k: Boltzmann constant

M_i ,M_j: Molecular weights for i and j (kg/kmol)

M_W: Molecular weight of the gas

n: volume exponent

P or Pi: Pressure (kPa)

P_1: Pressure of the inlet stream

P_2: Pressure of the exit stream

Pr: Prandtl number

q_i: Concentration of component i in the particle (kmol/kg)

q_i*: Equilibrium concentration of component i in the particle (kmol/kg)

q_e: Adsorbed amount of water on adsorbent (mol/g)

Re: Reynolds number

r_p: Adsorbent particle radius (m)

Sc: Schmidt number

Sh: Sherwood number

T: Temperature (K)

T_s/T_p: Adsorbent particle temperature (K)

T_w: Wall temperature (K)

t: Time (s)

U: Interstitial velocity (m/s)

W:Polytropic power for blower (kJ/h)

w_i: Loading of the adsorbed component over the maximum loading

y_i: Mole fraction of component i

z: Bed length (m)

ε_p: Particle porosity

ε_b: Bed porosity

$\varepsilon_{i,j}$: Molecular attraction energy

ρ_g: Gas phase density (kg/m^3)

ρ_p: Particle density (kg/m^3)

ρ_1:Density of the inlet stream

ρ_2:Density of the exit stream

μ: Gas viscosity (kg/m/s)

$\sigma_{i,j}$: Mean distance between molecules (°A)

τ : Tortuosity factor

Ω_D : Molecular collision function

ΔH_i : Heat of adsorption of component i(J/mol)

Figure captions:

Figure1. The sequence of cyclic process

Figure2. The thermodynamic diagrams for the system in terms of (a) x-y diagram and (b) ternary and residue curve map

Figure3. Comparison between experimental data and model for (a) diethyl ether and (b) ethanol for feed flow rate of 333 kmol/h

Figure4. Out-put of model in terms of (a) concentration of ethanol and diethyl ether as a function of time, (b) time interval of 27000 s for concentration of ethanol and diethyl ether as a function of adsorbent length and (c) temperature profile variation versus time at different length of bed for feed flow rate of 333 kmol/h

Figure5. Variation in (a) the Peclet number, (b) the Reynolds number, (c) maximum superficial velocity and (d) minimum fluidization velocity with timefor feed flow rate of 333 kmol/h

Figure6. Reaching to cyclic steady state condition for (a) ethanol and diethyl ether profiles, (b) water (steam) distribution and (c) temperature profile with time for feed flow rate of 333 kmol/h

Figure7. The average contribution of utilities cost from total operating costs

Figure 8. Interaction between parameters in terms of (a) A×C (for diethyl ether cyclic recovery), (b) A×D (for diethyl ether cyclic recovery), (c) B×C (for diethyl ether cyclic recovery), (d) D×C (for ethanol cyclic recovery), (e) B×C (for ethanol cyclic recovery), (f) A×B (for total operating), (g) A×C (for total operating), (h) B×C (for total operating)

Figure 9. The optimization path